AFRL-RX-TY-TR-2012-0032

SUPPORT TO A WIRELESS POWER SYSTEM DESIGN

Marcus D. Smith
Airbase Technologies Division
Air Force Research Laboratory
139 Barnes Drive, Suite 2
Tyndall Air Force Base, FL 32403-5323

Henry W. Brandhorst, Jr.
Carbon-Free Energy, LLC
1948 Stoneridge Drive
Auburn, AL 3680-7607

Contract No. FA4819-11-C-0010

December 2011

AIR FORCE RESEARCH LABORATORY
MATERIALS AND MANUFACTURING DIRECTORATE

■ **Air Force Materiel Command** ■ **United States Air Force** ■ **Tyndall Air Force Base, FL 32403-5323**

NOTICE AND SIGNATURE PAGE

Using Government drawings, specifications, or other data included in this document for any purpose other than Government procurement does not in any way obligate the U.S. Government. The fact that the Government formulated or supplied the drawings, specifications, or other data does not license the holder or any other person or corporation; or convey any rights or permission to manufacture, use, or sell any patented invention that may relate to them.

This report was cleared for public release by the 88th Air Base Wing Public Affairs Office at Wright Patterson Air Force Base, Ohio available to the general public, including foreign nationals. Copies may be obtained from the Defense Technical Information Center (DTIC) (http://www.dtic.mil).

AFRL-RX-TY-TR-2012-0032 HAS BEEN REVIEWED AND IS APPROVED FOR PUBLICATION IN ACCORDANCE WITH ASSIGNED DISTRIBUTION STATEMENT.

BOWEN.THOMAS.ARTHUR.1291059569
Digitally signed by BOWEN.THOMAS.ARTHUR.1291059569
DN: c=US, o=U.S. Government, ou=DoD, ou=PKI, ou=USAF, cn=BOWEN.THOMAS.ARTHUR.1291059569
Date: 2012.06.15 15:27:20 -05'00'

THOMAS A. BOWEN, 1st Lt, USAF
Work Unit Manager

SALAVANI.REZA.1230156944
Digitally signed by SALAVANI.REZA.1230156944
DN: c=US, o=U.S. Government, ou=DoD, ou=PKI, ou=USAF, cn=SALAVANI.REZA.1230156944
Date: 2012.06.19 11:16:52 -05'00'

REZA SALAVANI; DR-III, CIV
Program Manager

RHODES.ALBERT.N.III.1175488622
Digitally signed by RHODES.ALBERT.N.III.1175488622
DN: c=US, o=U.S. Government, ou=DoD, ou=PKI, ou=USAF, cn=RHODES.ALBERT.N.III.1175488622
Date: 2012.07.17 12:25:30 -05'00'

ALBERT N. RHODES, PhD
Chief, Airbase Technologies Division

This report is published in the interest of scientific and technical information exchange, and its publication does not constitute the Government's approval or disapproval of its ideas or findings.

REPORT DOCUMENTATION PAGE

Form Approved
OMB No. 0704-0188

PLEASE DO NOT RETURN YOUR FORM TO THE ABOVE ADDRESS.

1. REPORT DATE *(DD-MM-YYYY)*	2. REPORT TYPE	3. DATES COVERED *(From - To)*
21-DEC-2011	Final Technical Report	10-MAR-2011 -- 10-MAR-2012

4. TITLE AND SUBTITLE

Support to a Wireless Power System Design

5a. CONTRACT NUMBER

FA4819-11-C-0010

5b. GRANT NUMBER

5c. PROGRAM ELEMENT NUMBER

0909999F

6. AUTHOR(S)

Smith, Marcus D.; Brandhorst, Henry W.

5d. PROJECT NUMBER

GOVT

5e. TASK NUMBER

D0

5f. WORK UNIT NUMBER

QD102014

7. PERFORMING ORGANIZATION NAME(S) AND ADDRESS(ES)

Carbon-Free Energy, LLC
1948 Stoneridge Drive
Auburn, AL 36830-7607

8. PERFORMING ORGANIZATION REPORT NUMBER

9. SPONSORING/MONITORING AGENCY NAME(S) AND ADDRESS(ES)

Air Force Research Laboratory
Materials and Manufacturing Directorate
Airbase Technologies Division
139 Barnes Drive, Suite 2
Tyndall Air Force Base, FL 32403-5323

10. SPONSOR/MONITOR'S ACRONYM(S)

AFRL/RXQES

11. SPONSOR/MONITOR'S REPORT NUMBER(S)

AFRL-RX-TY-TR-2012-0032

12. DISTRIBUTION/AVAILABILITY STATEMENT

Distribution A: Approved for public release; distribution unlimited.

13. SUPPLEMENTARY NOTES

Ref Public Affairs Case # 88ABW-2012-4094, 25 July 2012. Document contains color images.

14. ABSTRACT

Power remote sensors or UGV at a non-trivial distance that would normally require personnel to replace batteries or refill generator liquid fuel reservoirs. To develop a laser wireless power transmission system using an infrared laser to send power to remote sensors (~1 km) using photovoltaic laser power converter cells.

15. SUBJECT TERMS

laser, wireless power transmission, band gap, matched semi conductor, laser power converter, GaAs

16. SECURITY CLASSIFICATION OF:			17. LIMITATION OF ABSTRACT	18. NUMBER OF PAGES	19a. NAME OF RESPONSIBLE PERSON
a. REPORT	b. ABSTRACT	c. THIS PAGE			Marcus D. Smith
U	U	U	UU	29	19b. TELEPHONE NUMBER *(Include area code)*

Reset

TABLE OF CONTENTS

LIST OF FIGURES

Page

LIST OF TABLES

Page

1. EXECUTIVE SUMMARY

In order to meet the increasing power demands of operations around the world, the U.S. Department of Defense has been exploring alternate sources of power beyond conventional land lines or diesel-electric generators. The latter have proven problematic in hostile environments where the supply chain can be disrupted by adversary actions and a great many lives are lost transporting diesel fuel. Fixed land power lines pose additional constraints and vulnerabilities.

Photovoltaic power systems offer a convenient source of power in sunny climates, but such power is generally variable on a daily basis. A fourth option that appears to offset some of these disadvantages is the use of wireless power transmission. Wireless Power Transmission (WPT) is a technology that offers a significant tactical advantage for activities such as remotely powering perimeter security sensors, recharging in-flight Unmanned Aerial Vehicles (UAVs), and a host of other.

This report describes the planning, laser selection and testing, laser hazard analysis, the solar cell selection and its testing, the data acquisition system and experimental results of a short field test. The 2.5 kW DILAS laser operated at 810 nm and had an expected beam size at 100 m of 0.315 m wide by 0.29 m high. At the intended 1 km distance, the beam size was expected to be 2.5 m wide by 2.0 m high. This laser had multiple solid state beaming units causing the beam to be made up of multiple overlapping ellipses. This led to significant beam non-uniformity which adversely affected test results. The test site is located at the Eglin Air Force Base and because of the hazards involved in outdoor laser testing; the American National Standard for Safe Use of Lasers Outdoors (ANSI Z136.6-2005) document was followed. This facility offers a maximum range of 1 km. This test was limited to 100 m for these initial tests for safety reasons.

The solar array was made from gallium arsenide (GaAs) solar cells with two GaAs junctions. There were 42 cells in the array with 40 being active. They were arranged in five 8-cell series strings. When tested indoors, this array produced more than 200 W. Because the test distance was limited to 100 m, the laser beam size was smaller than the array. This necessitated a major change in the experiment. The array was turned 90° on its side and the three non-illuminated series strings were disconnected.

The test results produced only limited current/power from the array. This was caused by major non-uniformities in the laser beam. This non-uniformity caused some of the cells in the series string to receive less light than others. Because the cell with the least output in a series string controls the output, the results were disappointing. However, the lessons learned are most helpful in planning future tests.

These lessons include the need for close collaboration between the laser range safety officers and test planners to ensure all test plans are endorsed by all. Secondly, more extensive laboratory testing of the laser with the array along with detailed laser beam profile measurements are critical to success. This will entail using indoor test sites that allow sufficient distance to uncover any issues like those uncovered in this test. Future testing that takes these lessons into account should produce excellent results that confirm the viability of power transfer to remote locations or sites by beamed laser power.

2. INTRODUCTION

The U.S. Department of Defense has continually increasing energy requirements as it fulfills its mission around the world. The major burden of producing the power has resided with diesel-electric power generators. Recently photovoltaic power systems are being used to reduce the amount of diesel fuel. The latter have proven problematic in hostile environments where the supply chain can be disrupted by adversary actions. Fixed land power lines pose additional constraints and vulnerabilities. Photovoltaic power systems offer a convenient source of power in sunny climates, but such power is generally variable on a daily basis. However, a new option is emerging that may reduce the demand for diesel fuel and/or fixed power lines. This option is to use wireless power beaming where the source is a near-infrared laser and the receiver is a tuned solar cell. The source of the laser beam could be on an airplane, a spacecraft or a ship, so long as the receiving array is within line-of-sight of the source. This paper will describe the laser source and its characteristics, the photovoltaic receiver and its characterization, laboratory test results, requirements for outdoor testing and preliminary results of an outdoor test.

Wireless power transmission (WPT) is a technology that offers a significant tactical advantage for activities such as remotely powering perimeter security sensors, recharging in-flight unmanned aerial vehicles (UAVs) and a host of other applications. This report summarizes the steps leading to a ground test of laser power beaming. Various parts of this report cover the selection criteria for choosing the operational wavelength of the wireless power link, technologies chosen for both transmitting and receiving power at that wavelength, characterization results of the receiver material, and a discussion of the lessons learned in the initial ground test.

Selecting a transmission wavelength is a complicated issue because several factors have to be considered such as wavelength-dependent transmission through the atmosphere, divergence of the laser beam, Technology Readiness Level (TRL) of both the transmitter and receiver technologies, efficiencies of the link components, tolerance to extremes in operating conditions, portability, weight, safety, interference with other military systems, etc. Different portions of the electromagnetic spectrum offer unique advantages and disadvantages. Wave propagation or transmittance is affected by the various gases in the atmosphere that absorb, refract, and reflect electromagnetic energy. These effects are far from uniform across the spectrum and are different for each atmospheric component. There are certain portions of the spectrum that pass nearly all of the energy resulting in a high transmittance level. After a careful review of these factors, a wavelength in the near infrared (NIR) spectrum was chosen (808 nm). More details will follow.

Photon sensitive semiconductor junctions are used to convert this beamed light energy into electricity. All photon sensitive semiconductor junctions do not respond to the same portion of the light spectrum with high efficiency. The band-gap energy requirement of a semiconductor is the energy required to boost an electron from the valance band to the conduction band. For light in the NIR, GaAs-based solar cells are the best because the photon energy of a portion of this spectrum (800 nm to 870 nm) coincides with the peak band-gap energy of GaAs. Another ideal property of GaAs is that it is a direct band-gap semiconductor which means that the light falling on the device near the band gap edge is highly absorbed. This leads to high efficiency of conversion.

Other semiconductor junctions such as silicon (Si) have an indirect band gap and therefore the efficiency of conversion of light near its band edge is less efficient. It is the most widely available and low cost solar cell, so it use requires a careful analysis. A decision on whether to use Si solar cells for this test depends on the atmospheric transmission in this spectral region and will be discussed further.

Thus the two primary criteria for a successful laser beamed energy transmission experiment have been fulfilled: the laser light source must have high transmission through the atmosphere along with a photovoltaic (PV) receiver cell that can absorb that light and convert it into useful power with high efficiency. Then the third issue that must be considered is the safe design of a ground test. Lasers are very dangerous and all aspects of range safety must be studied and approval for the test from the Range Safety Officer (RSO) must be obtained before any testing.

Finally, given approval for the test, substantial test equipment must be assembled and verified, the range set up and the laser source and solar cell receiver must be positioned perfectly so no scattered laser light goes astray. Finally, a stepwise increase of distance between the laser and the test array will lead to results that can be used for projecting the usefulness of laser power beaming for a range of applications.

In this report we will cover the laser selection and testing, the solar cell selection and array fabrication/testing, the safety issues, the results of the first ground test and lessons learned.

3. METHODS, ASSUMPTIONS, AND PROCEDURES

3.1. Atmospheric Transmission and the Selection of a Laser Wavelength

The atmosphere is composed of various gases all of which have particular absorption bands. Hence selection of a laser wavelength matched to a solar cell must take this into consideration. There are two spectral windows that are particularly relevant for commonly available solar cells. Figure 1 shows the atmospheric transmission spectrum beyond 900 nm, and the atmosphere is relatively transparent beyond 1000 nm [1]. Although this appears to match the band gap of the silicon solar cell, this is a bit misleading because the peak in the silicon solar cell response comes at about 900-950 nm. These would be the most ideal wavelengths to use for silicon, but, as shown in Fig. 1, atmospheric absorption is too high in this region to make Si solar cells a strong competitor. Thus they were eliminated from consideration for this test.

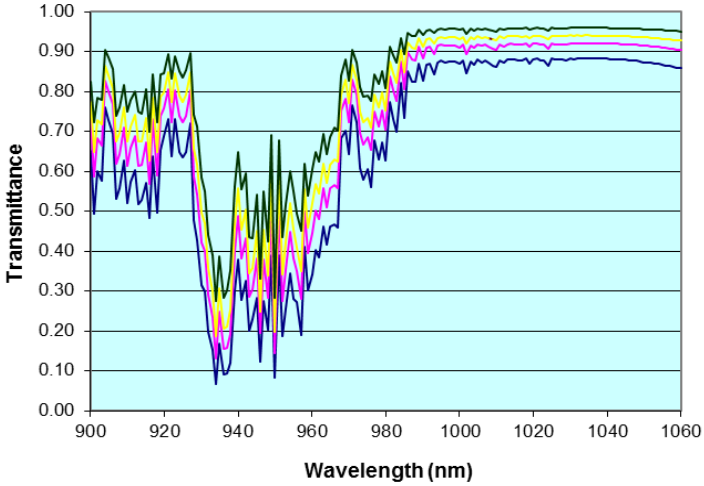

Figure 1. Atmospheric Transmission Spectrum beyond 900 nm

Figure 2 shows the wavelength region from 800 nm to 900 nm in the near infrared as a function of air mass vertically through the atmosphere. At sea level, a horizontal beam would be traversing through about 20 air masses (AM), so even small absorption will be important. However, this test is to be carried out over a distance of only 1 km, so do these spectra have any pertinence? To make the comparison, we'll make a simplifying assumption that the atmospheric composition is the same in a vertical column of air as in a horizontal column of the same area. A vertical column of air 1 cm^2 in area weighs about 1,030g according to the US Standard Atmosphere 1976. Similarly, the density of air at sea level is 1.204 kg/m^3. Using this value, a 1 cm^2 column of air at sea level would be about 10 km in length. Therefore, we would expect less absorption (about 9%) in the 1 km path length. Thus the AM1 spectrum can be a conservative spectral distribution for our test. There is an excellent window in the region between 840 and 890 nm. This wavelength range corresponds to cells with band gaps between 1.39 and 1.47 eV. An ideal solar cell in this range is GaAs with a band gap at room temperature of 1.42 eV. A second possible region is between 800 and 810 nm. Selection of a laser with this wavelength will also match a GaAs solar cell, but may not reach the highest possible efficiency.

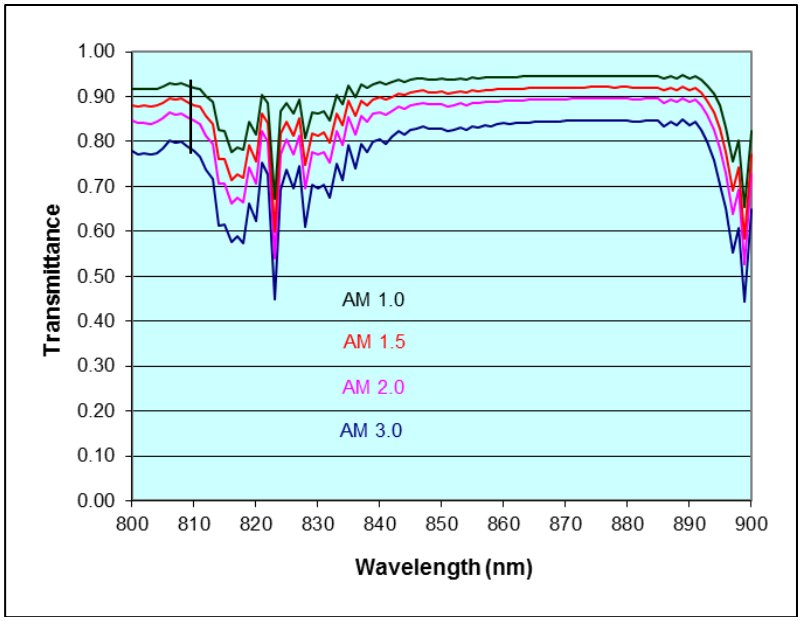

Figure 2. Atmospheric Transmission between 800 nm and 900 nm

As previously stated, various atmospheric conditions can affect the window in the atmosphere for the 810 nm laser beam. Figure 1 and Figure 2 show a typical calculation of atmospheric transmission with air mass [1]. Figure 3 defines air mass 1 as the path through the atmosphere when the light source is directly overhead. Air mass 2 is when the source is at an angle of about 60° from the vertical to the receiver. Air mass 3 occurs at 70.5°. Equation 1 is a general equation for computing air mass and takes into account the earth's curvature:

$$AM = \frac{1}{\cos\theta + 0.50572(96.07995-\theta)^{-1.36364}} \quad (1)$$

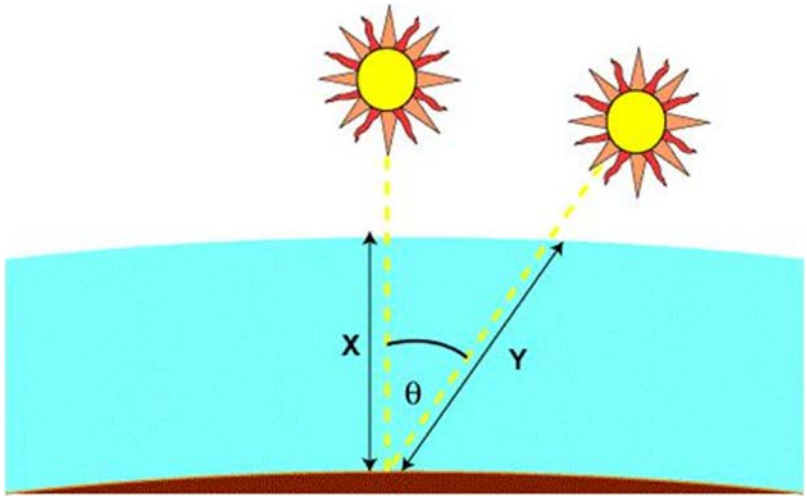

Figure 3: Depiction of Air Mass

The black vertical line in Figure 2 represents the 810 nm laser wavelength. As shown, this wavelength is right on the edge of an atmospheric absorption band. This band is due to weak absorption by carbon dioxide (CO_2) and water (H_2O) molecules. The exact composition of the atmosphere at the time of the test will impact the depth and breadth of this absorption band. Given that this is a ground level test, both humidity and atmospheric turbulence will affect the transmission of the laser beam. Turbulence arises due to heating of the earth leading to heating of the atmosphere. Small variations in temperature lead to small variations in refractive index which is the cause of turbulence.

Turbulence effects can also have a serious impact on laser power beaming tests. The blooming effects will distort the laser beam leading to beam spread and wander. Wind speed will be a factor as well. Thus it would be best to perform testing on a day with low wind speeds and at times when heating of the earth by the sun is minimal.

During testing, all the standard weather information was monitored with a standard weather station: ambient temperature, wind speed and direction, relative humidity, dew point, barometric pressure and global solar irradiance with a pyranometer. The equipment used was obtained from NovaLynx Corporation, P.O. Box 240, Grass Valley, CA 95945. Most of these parameters except for turbidity are usually included in these weather stations. Turbidity measurements usually require a special instrument.

Atmospheric measurements will be important for interpreting the results. For the purposes of this test, the atmospheric mixing ratio should be calculated for each data point and for each distance. The calculations are complex, but are simplified by using a web site for calculating the equations developed by NOAA: http://www.srh.noaa.gov/epz/?n=wxcalc.

3.2. Selection of the Laser and its Characterization

3.2.1. Laser Beam Source

A high power, high brightness multipurpose diode laser was purchased from DILAS Diode Laser, Inc., 9070 South Rita Road, Suite 1500, Tucson, AZ 85747, U.S.A., for this experiment. It has an input power level of 2550 W with an output at the aperture of 2046 W at 90 A current. The 810 nm, continuous wave (CW) laser module is made of two 15 bar water-cooled stacks. The beams are interleaved to achieve high brightness and the output beam has a top hat profile. The laser is equipped with a custom expansion module. Figure 4 shows the front part of the laser with the beam expansion module. The beam divergence is 3.96 mrad × 2.93 mrad.

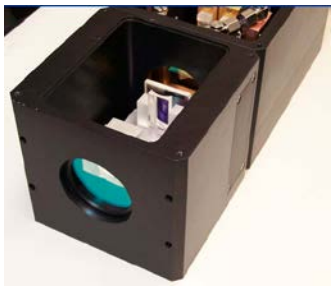

Figure 4. DILAS Laser Showing Beam Expansion Module

The power supply and water cooling system is contained in one portable cabinet. Special effort has been made to ensure pure water supply for cooling to prevent fouling and/or clogging and subsequent damage to the laser. The DILAS laser is mounted on a heavy-duty tripod that can be aligned horizontally and vertically. Because the 810 nm high power beam is invisible to the eye, a 532 nm aiming laser is mounted beside it. This aiming laser is a Hercules 375 CW laser made by Laserglow Technologies, 5 Adrian Avenue, Toronto, ON, M6N 5G4, Canada. Its average power is 399 mW with an elliptical beam profile. According to documentation, the beam divergence is 0.2 mrad × 0.2 mrad without a beam expander installed. Test reports and hazard analyses of both lasers are presented in Appendix B.

These test results indicate that the intensity of the laser at a distance of 1 km will be about 28 mW/cm^2 – or about 25% as intense as sunlight. It will be bright enough to produce an expected power output of about 25 W from the PV array. On the other hand, the aiming laser spot size at 1 km has been reported by the manufacturer to be 30 mm with the beam expander installed. Because the target area is 1 ft. × 2 ft. (30.5 cm × 61 cm) the aiming should have sufficient accuracy. The adjustments on the tripod are somewhat coarse, but appear to be satisfactory, but no test at distance has been made to confirm the accuracy of pointing.

Appendices A and B include more detailed information on an assessment by the Eglin AFB laser safety experts about the hazards of the initial 810 nm beam as well as the reflected beam. Appendix B also provides laser test and hazard analysis for this laser using the LHAZ software. This software was developed by the AFRL and determines the optical and skin hazard distances that are critical for safe operation of the laser in tests. As will be noted in the next section, the reflectivity of the solar array is less than 5% at 810 nm. Thus, at most, the reflected beam would only have a power level of 53 W. As shown in that analysis, this is not a hazard at the beaming source.

In addition, the test site must be equipped with sun-blind laser power meters that can record power levels up to 3 kW/m^2. Because of the small beam divergence of the DILAS laser, the test array must be moved to a location where its area is fully illuminated by the 810 nm beam. Failure to illuminate all of the solar cells in the array will lead to erroneous measurements. Thus a series of calibration measurements must be made of the area of the 810 nm beam as a function of distance from the source. In addition, the spread of the beam can be controlled by moving the beam expander optics to change the divergence. These measurements will have to be performed in the field.

The following characteristics of the CW laser had to be provided to the RSO prior to testing: wavelength, beam profile (circular or elliptical), beam distribution (Gaussian or Top Hat), power, beam geometry (divergence, diameter at waist, extended source size) and total on-time of the system. The 810 nm, 2.5 kW DILAS laser used in these tests had adjustable optics that allowed some significant degree of control of the beam profile. The nominal divergence of the laser is 2.15 mrad wide × 1.9 mrad but is increased to 3.96 mrad wide × 2.93 mrad wide using the beam expander module. The ability to vary the beam divergence led to a degree of uncertainty in actual beam size, and a concern from the RSO that led to the limitation on beaming distance. Figure 5 shows the power output of the DILAS laser with current. During these field tests the power level of the laser was 285 W determined from this calibration curve.

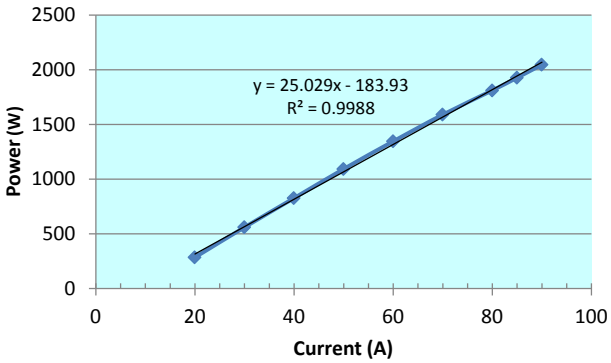

Figure 5. Laser Calibration Curve

Based on the laser tests described above, Figure 6 shows the beam pattern that is expected with beaming distance for the field tests. The beam profile at 1 km will be 2.25 m wide × 2 m high. At 100 m the size will be about 0.315 m wide × 0.29 m high. The expected beam profile with respect to the test solar array will be covered in the next section. There was no ability to measure the beam profile under the range safety considerations during this test. This limited the ability to demonstrate the efficiency of the system.

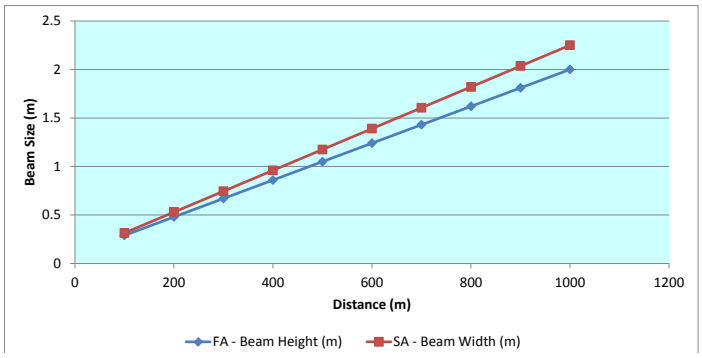

Figure 6. Laser Beam Size with Distance

3.3. Selection of the Solar Cell and Testing of the Array

With the atmospheric transmission in hand, the next step is to look at the characteristics of a GaAs solar cell [1]. Figure 7 shows the effects of temperature on the band gap and power point of a GaAs solar cell. This curve is important because the solar cell will heat up under the laser beam. As it heats, the band gap will shift (and the cell voltage will decrease). Thus the optimum laser wavelength will also shift. For the tests reported in [1] a laser wavelength of 859 nm was used. This laser wavelength was selected based on the maximum operating temperature of the cell of 90 °C. It is also important to note that this cell is a single junction device. A III-V-based multijunction solar cell will not respond well to a single laser wavelength because all junctions must be excited by illumination. If one junction is not illuminated, it is likely that the cell/array will have no output. In that series of tests, we produced over 35% efficiency with the laser on a GaAs cell. Thus the single junction GaAs solar cell is the basis for this ground test.

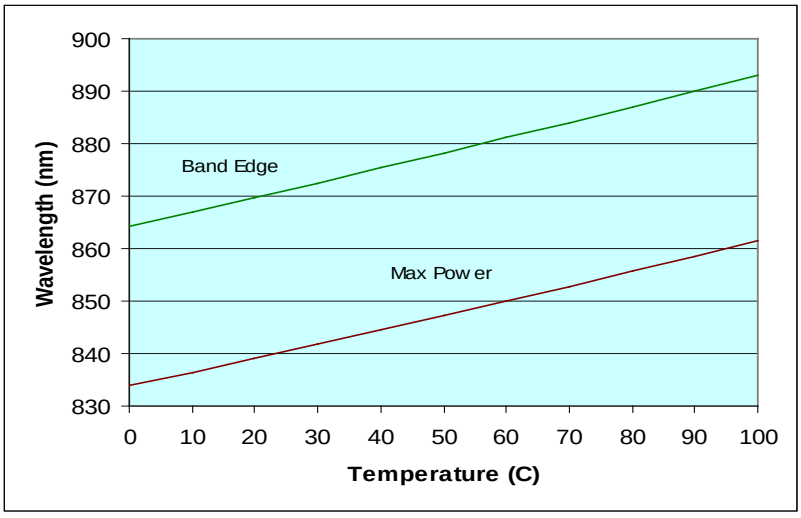

Figure 7. Effect of Temperature on the Band

GaAs solar cell samples were obtained from two space solar cell manufacturers (Emcore and Spectrolab) and exposed to a tunable Titanium:Sapphire (Ti:Sapphire) laser. The bandwidth of the laser was less than 7 nm full width at half maximum (FWHM) across the entire operational wavelength range. Maximum continuous power at the output aperture of the laser was 4.2 watts at 830 nm. Power at the sample was controlled using a Fresnel Rhomb (¼ wave) and a polarizing cube combination. All optical powers reported in the results are relative to the absolute power measured at a laser wavelength setting of 830 nm. A beam splitter placed after the polarizing cube (before the shutter) was used to monitor a lower power sample of the test beam. Measurements were made in the reference beam continuously during each exposure for each test condition. Before experiments began, the reflection (R) and transmission (T) of the beam splitter was characterized over the operational power range of the laser. The ratio (T/R) was found to be constant over this power range. Smith, et al [2], provides extensive additional detail on the laser/cell testing that was performed and the methodology for selection of the solar cells for testing. Selected parts of that report are presented below.

Measurements included wavelength response, junction saturation, area of illumination, surface response homogeneity, temperature characteristics and damage threshold with the laser set to a wavelength of 808 nm. Because these tests were run at different organizations, different laser wavelengths have been used. It's important to note that all the wavelengths (859, 830, 810 and 808 nm) are within the response band of the GaAs solar cells and will show only small differences in performance. Figure 8 shows a comparison of the efficiency of two cells supplied by different manufacturers [2]. It is important to note that one cell produced a higher efficiency at high intensity, whereas the other had a lower efficiency at a lower intensity (and the efficiency reduced as the intensity increased as determined with other tests). Cell B.1 had the highest efficiency consistently in all tests. In general both cells responded in the same way with temperature testing from 10 °C to 130 °C. The cells were measured across a fixed 6.2 Ω load. Based on these tests, Manufacturer B was selected to supply the cells for the test array because they showed the highest efficiency of approximately 45%. No differences were noted in the other tests.

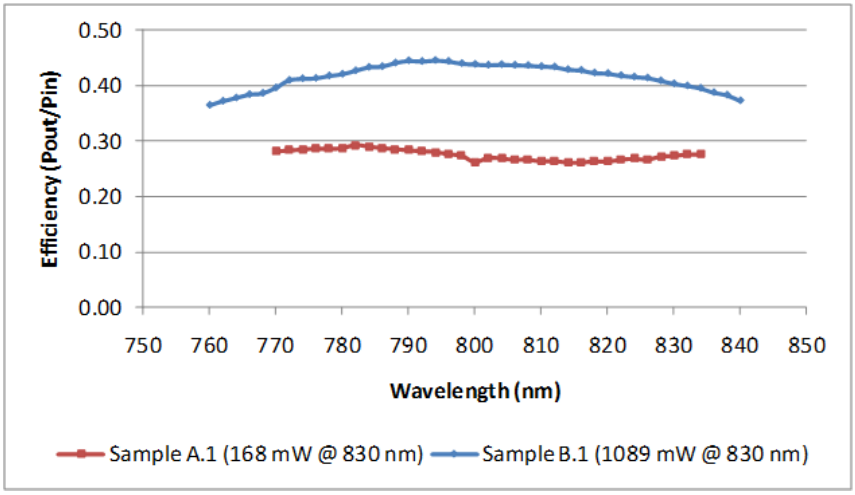

Figure 8. Solar Cell Efficiency Measurements

The solar array for this test was supplied by Spectrolab/Boeing. Spectrolab fabricated the solar cells and Boeing assembled them into an array for these tests. The solar cells are essentially two GaAs solar cells in series, hence will perform like a single junction solar cell for the purposes of this test. When tested under the 808 nm laser irradiation, individual cells had efficiencies of about 50%. Individual cells vary in performance and when put into an array, actual efficiency may be reduced. These cells are standard size cells (26.6 cm^2) used in spacecraft.

The antireflection coating is tailored such that it has a minimum reflectivity at 810 nm of about 4% as shown in Figure 9. This curve shows only the wavelength range of interest to this study. It is interesting to note that the bare cell has a reflectance around 2% over much of this wavelength range.

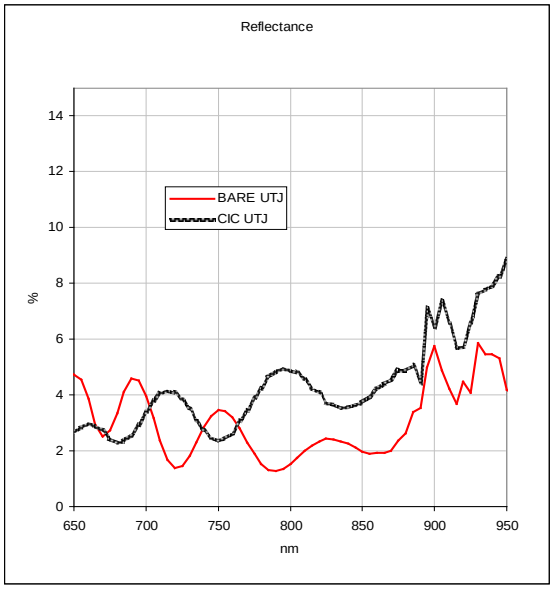

Figure 9. Reflectivity of GaAs Solar Cell

Initially, the manufactured solar cells were connected into an array with six cells in series and five parallel rows for a total of 30 cells. Figure 10 shows a planned layout of the cells. The cells are mounted on a frame made from 80-20 standard 1 in × 1 in T-slot extrusions. The framework has with vertically-oriented fins to aid in cell cooling (Figure 11). In addition, interconnecting the cells has to take into account the laser beam non-uniformity across the array. For example, if the six cells were connected in series and the five columns in parallel, significant power losses would happen. This is because in a series string of solar cells, the cell with the least illumination generates the least current. Hence the output of that string is limited to that lowest value. Using the energy distribution of the laser beam at a 1 km distance, obtained from DILAS, an interconnection scheme was designed to minimize the impact of beam non-uniformity. That design was implemented and the cells were interconnected accordingly.

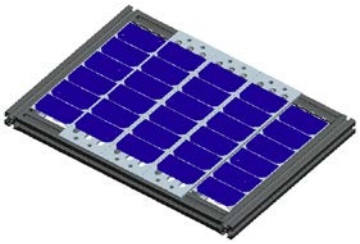

Figure 10. Layout of GaAs Cells on an Aluminum Extrusion Framework

Figure 11. Rear View of Laser Solar Cell Array Framework

This array did not produce the goal output of 200 W under laser illumination. Therefore, two additional six-cell strings were fabricated and mounted as “wings” on each side of the existing panel. It was determined that two of these additional cells were not functioning hence they had to be excluded from the array. This was done simply by putting a jumper wire around them. Figure 12 shows a picture of the final array.

Figure 12. Finished GaAs Array for Laser Testing

With this modification, a new interconnection scheme was developed using the laser beam distribution shown in Figure 13. This figure includes the approximate size of the GaAs test array shown in Figure 12. Within the rectangular area, the beam intensity varies by about a factor of 2.5x. This will have an effect on the overall performance of this array. Given this intensity profile, a new interconnections design was developed and is shown in Figure 14. It is a very complex design and field testing will determine its efficacy. Part of the complexity occurred because two of the cells in the new wings were not functioning (shown in grey). They were jumped out of the circuits. The color coding is used to show those cells that are connected in series. (The complex wiring pattern is not shown.) Thus the cells numbered from 1 to 10 are in series. For ease of identifying cells, all cells with the same number have the same color. The cells noted with a "0" are shorted out of the circuit. This pattern results in four rows connected in parallel each with ten cells in series for a total of 40 active cells. The colors are a means of displaying the distribution of the cells across the array. This distribution was intended to mitigate the impact of beam non-uniformity as noted above.

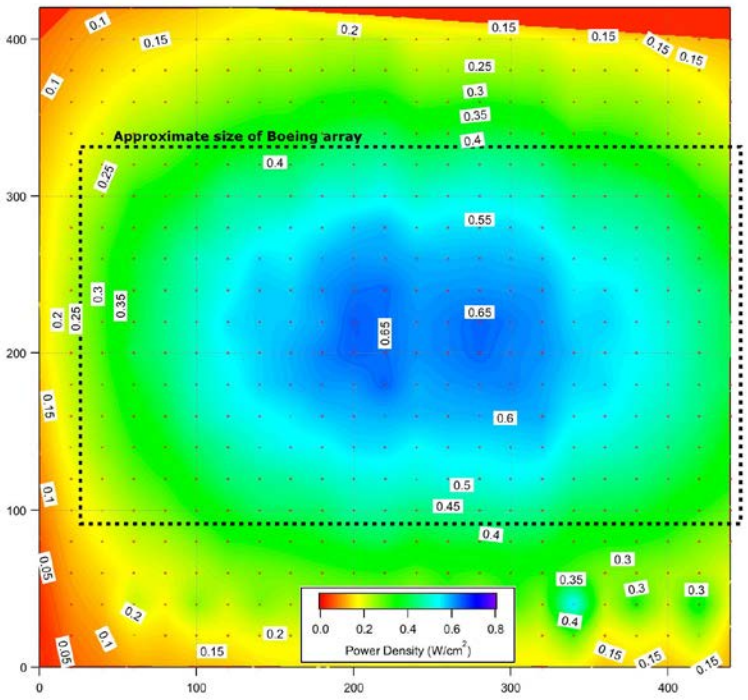

Figure 13. Measured Profile of the DILAS 810 nm Laser Beam

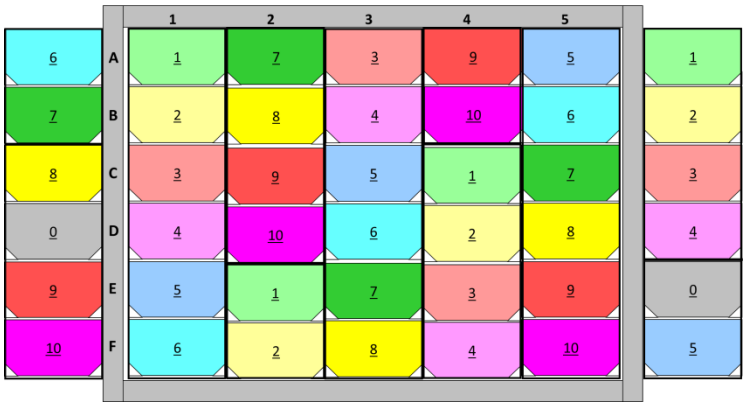

Figure 14. Schematic of Interconnected GaAs Cells

3.3.1. Laboratory Testing of Array with 808 nm Laser

The upgraded, 7 rail (6 cells per rail) solar array was tested to confirm its capability of producing at least 200 W of electrical output under illumination by 808 nm laser light. This was the only laser wavelength available for this indoor test. Although it is not the same as the 2.5 kW DILAS laser used in outdoor testing, the difference is not significant due to the high absorption of the GaAs solar cells in this region of the spectrum. Because the array had been upgraded to include 2 more rails than during previous testing, an optical concentrator had to be added in order to provide adequate power density on the outer rails. The array with concentrator is shown in Figure 15, and the illuminated array with concentrator is shown in Figure 16. Although the eye cannot see this light wavelength, the camera can, hence the illuminated picture clearly shows the beam.

Figure 15. Test Array with Mirrors

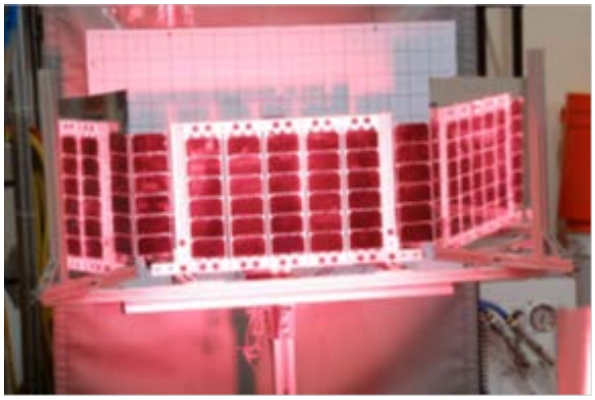

Figure 16. Array Under Laser Illumination

The upgraded array also included 5 small fans hooked in parallel with the output electrical connections. These fans were able to provide adequate airflow to keep the array temperature in the low-to-mid 40 °C range. The upgraded array had been re-wired to put 10 cells in series, such that the array produced maximum power at around 17–18 V. Based on multiple runs, the array was able to produce more than the minimum required 200 W. The power going to run the cooling fans was not included. Optical power density was not measured, but is estimated as averaging around 0.4 W/cm^2. A representative I-V curve for the array is shown in Figure 17. The

peak power of this array was 240 W under this laser illumination level. The measurement sequence took approximately 40 seconds. Four temperature sensors in various locations around the test article recorded temperatures that ranged from initial starting temperatures between 33.5 °C and 42.5 °C. By the end of the test the temperatures had **o**nly increased to 35 °C and 44 °C. Averaging all thermocouples gave a range from 38.25 °C to 39.5 °C. Thus the array was ready for field testing.

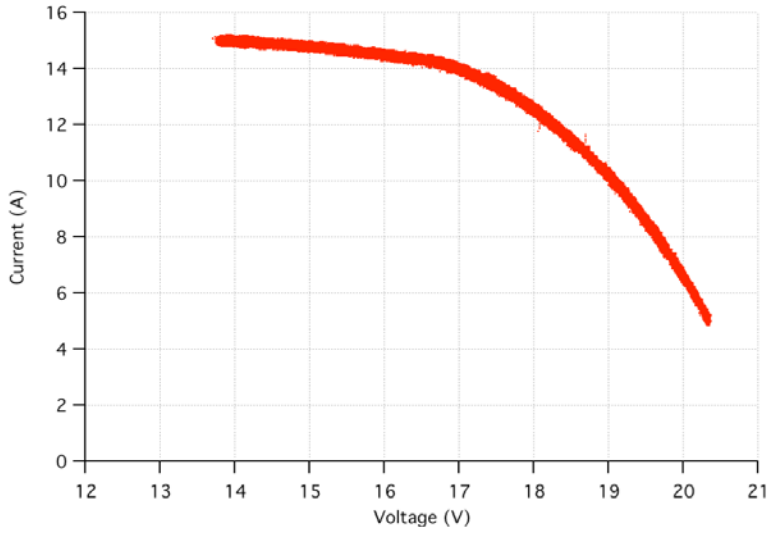

Figure 17. I-V Curve of the Test Array

3.4. Laser Safety Issues

Whenever laser power beaming experiments are planned, safety issues become predominant. Safety issue concerns increase with increases in laser power. With the 2.5 kW DILAS laser used in this test, its power level raises safety issues that must be addressed and are briefly covered here. References [3] and [4] and Appendices A and B contain extensive coverage of the potential safety concerns and what safeguards can be implemented to ensure the safe usage of laser beamed power technology.

The top issues are noted below. Extensive U.S. Government regulations cover all these areas and will not be covered here [3, 4]. The top three issues are: eye safety, burns and tissue heating, and fire.

- **Eye-Safety:** Intense laser beams can damage the eye. Hazards include direct viewing of the beam source or exposure to reflections.
- **Burns &Tissue-Heating:** Exposure to intense laser or microwave beams --or their side lobes--can cause first, second, or even third degree burns. As with eye safety, the hazards include exposure to direct or reflected beams.
- **Fire:** Intense laser beams can ignite fires in foliage, clothing, or other materials.

Safe operation of hazardous technologies usually relies on a combination of design features, protective equipment, and operating procedures and training. These are often codified in government or industry standards. Power beaming is no exception. The use of high power lasers

and microwaves is already widespread in defense and in industry. As a result, industry groups have already developed and validated standards for safely using lasers and microwaves in situations similar to power beaming:

- American National Standards Institute (ANSI) Z136.6, American National Standard for Safe Use of Lasers Outdoors.
- AFRL/RH is the recognized leader in standards development for laser use in the U.S. They have conducted extensive research into the effects of lasers exposure to human beings including significant animal testing.

The first line of defense is to design power beaming systems that prevent or minimize human contact with hazardous radiation. References [3] and [4] and ANSI Z136.6 describe in detail four tenets of safe design: intensity limits, interlock protocols, elevated beam paths and warning systems.

4. RESULTS AND DISCUSSION

4.1. Ground Test Description and Results

The test site is located at Eglin Air Force Base, FL and the layout is shown in Figure 18. Because of the dangers involved in outdoor laser testing, ANSI Z136.6-2005 was followed. This facility offers a maximum range of 1 km. This test was constrained to only 100 m for initial testing and to ensure safety as noted above.

Figure 18. View of Laser Test Range at Eglin AFB, FL

The following equipment was used to conduct the tests. The 2.5 kW, 810 nm, DILAS laser and power supply as noted above, a Temotek laser chiller, a 10 kW programmable power supply, the solar array receiver and a 532 nm Nd/YAG green diode laser for aligning the DILAS laser to the target.

Because of the need for laser safety, the nominal ocular hazard distance (NOHD) and the nominal skin hazard distances (NSHD) were determined and are shown in Table 1. Personnel were required to stay outside of the NOHD and NSHD at all times.

Table 1. Optical Hazard Calculations

Laser	NOHD	NSHD
532 nm	3250 ft. (991 m)	330 ft. (100 m)
810 nm	3 miles (4.8 km)	1250 ft. (381 m)

A backstop was used to capture any laser radiation that was not directed onto the target. It was 8 ft high × 8 ft wide to capture that energy. The surface was painted black with thermal-resistant paint. Figure 19 shows the backstop with the automated data acquisition system for obtaining the array I-V curve under laser irradiation.

Figure 19. I-V Curve Tracer Behind Backstop

Figure 20 shows the Hercules Corporation portable green aiming laser (output power 250–800 mW at 532 nm) on the test array. This also shows one of the problems using a green pointer laser to align the infrared laser. The green laser was attached to the top of the DILAS 2.5 kW laser. It had not been bore sighted to ensure it exactly matched the laser beam point of aim. Hence there was a misalignment problem that raised a safety concern. Although this was not a major barrier at the 100 m distance, it was an issue for greater distances. Hence the RSO limited the test to the 100 m distance and did not allow the 1 km test to take place. Figure 21 shows a photograph of the 810 nm laser beam on the backstop to confirm divergence measurements. The image can be captured by the camera because it "sees" this NIR light whereas the eye cannot. This image confirmed that the size of the beam at 100 m is close to the expected values of 0.315 m wide by 0.29 m high as shown in Figure 13. The solar array has been lowered to the ground. The metal frame of the solar array had been treated to reduce any back reflections that may occur. This is critical to prevent eye or skin damage to personnel.

Figure 20. 532 nm Aiming Laser

Figure 21. Beam Profile at 100 m

Because of restrictions at the Eglin test site, only a limited amount of data was obtained. Figure 22 shows a screen capture of one of the data runs. The picture in the upper left is an image of the 810 nm laser beam on the target array. The data system recorded temperature data from four thermocouples spaced across the array, the I-V curve data, weather station data and laser beam intensity. The I-V curve shown is from an initial calibration run and not the field test. During the test, cell temperatures rose only a few degrees due to the short illumination times.

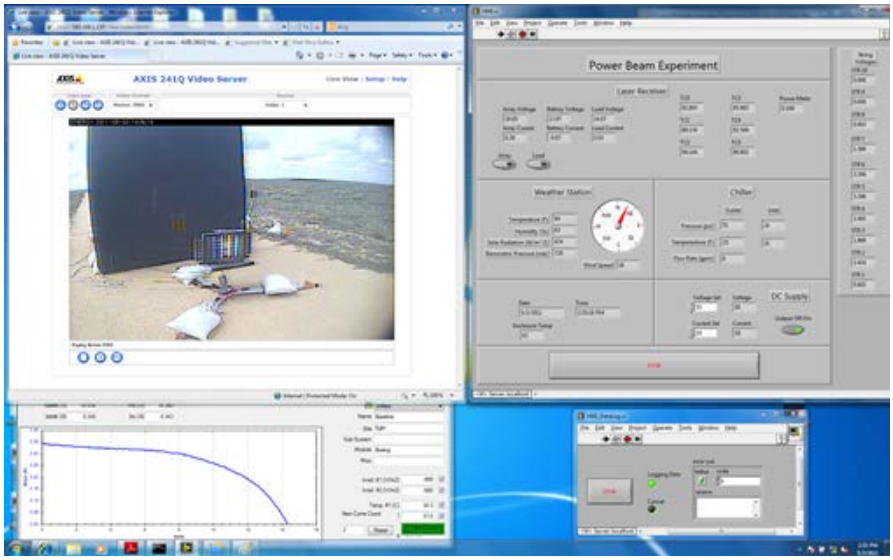

Figure 22. Laser Test Screen

According to laboratory test results, at a distance of 100 m, the laser beam should cover an area of approximately 0.315 m × 0.29 m or 914 cm^2. Given the current to the laser of 20 A, the beam power output should be at 285 W. Combining these values provides a beam power density of 0.312 W/cm^2. However, the intensity was not measured in the test plane so this power density is speculative. This beam area is much less than the area of the solar array, so some of the strings of cells were not illuminated and others were partially or fully illuminated. To help overcome this limitation, the solar array was demounted from the tripod and placed on the ground as shown in Figure 21 (and not as displayed in the photo shown in the screen shot in Figure 22). This was done to have the beam illuminate a single string of cells. The resulting array configuration is shown in Figure 23. As shown by the white arrows, String 1 occupies grid column 1 and most of 2. All of the rest of the strings were disconnected to prevent unwanted loading on this single active string.

If the actual beam area was as expected, then the cell string should have been fully illuminated. Because of the intensity variation across the area of the beam, some cells were receiving less than half the full beam intensity as shown in Figure 14. In addition, the situation was more complicated because the laser head contains multiple beaming units. This led to a beam that consisted of multiple overlapping ellipses as shown in Figure 24. Thus the intensity variation across this string of cells was much larger than expected. A single cell in the series string could be irradiated by a more intense laser beam and the neighboring cell might receive less than one-

third that intensity. Because the output of the string of solar cells will be limited by the cell with the lowest amount of current generated by the laser beam, the array output will be decreased.

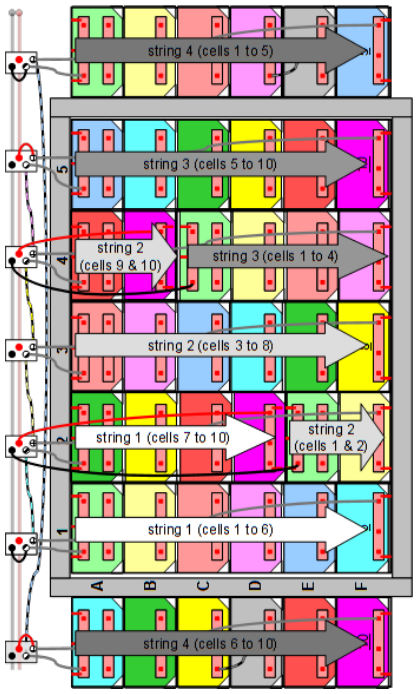

Figure 23. Array Orientation during Final Test

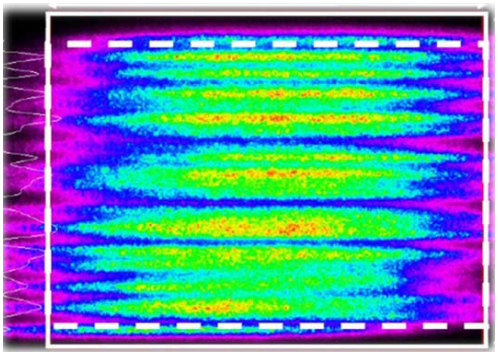

Figure 24. Image of Laser Beam at Target

The most likely scenario is this: Some cells are brightly illuminated (e.g. column 1), but some are dimly illuminated (e.g. column 2, in the dim zone between sub-beams). Each cell may have a range of laser intensity shining on it. It was not possible to obtain the beam profile during the test. The bright cells produce high current, but the dim cells produce little. The excess current produced by the bright cells is blocked and much of the power is wasted.

Given the previous assumptions, an estimate of the expected output of the array was made. Based on the ground testing results shown in Figure 17 the array produced an Isc of 15 A under a laser beam estimated at 0.4 W/cm^2. The estimated beam power density in this ground test was 0.312 W/cm^2 as presented above. With those values, the current of the array should have been 11.8 A. The observed current at the maximum power point was about 2 A suggesting that there were substantial additional losses amounting to 75% of the expected current. These losses were believed due to beam non-uniformity as described above. Given the total cell area in the string of 366 cm^2 the expected output should have been about 114 W. Unfortuantely, the observed power output was about 25 W (under these conditions). This 78% loss in power correlates well with the loss in current within measurement accuracy. Thus, the measured efficiency of the array was only 21.9%. This was less than half the expected efficiency as determined from individual cell tests noted in Figure 8. The limitations and requirements of the test site contributed to these discrepancies and the tests could not be repeated because time at the site had expired.

4.2. Lessons Learned

First, close collaboration with the laser RSO and personnel is essential. Their knowledge of the details of the laser, the test array and the possible optical hazards is critical to ensure a successful test. Because the green laser was not precisely bore-sighted with the DILAS laser, the RSO would not permit beaming over a longer distance. In addition, design of the backstop and concerns over the long distance performance of the laser contributed to the test limitations.

Secondly, extensive laboratory testing of the laser with the array and detailed beam profile measurements with a range of laser optics settings is required for successful testing. In this test the non-uniformity of the laser beam at the test target shown in Figure 24 contributed substantially to the inability of the solar array to produce the expected amount of power. Unfortunately, indoor test sites often do not have the length needed to resolve these potential issues. Thus, in the future a defined requirement for beam uniformity over a range of distances must be established and verified.

5. CONCLUSIONS

The major finding of this effort is that outdoor testing on a tightly controlled laser range limited the range of measurements that could be done. Without beam profile measurements at the array, the size, intensity or the uniformity of the beam could not be determined. Because of the potential misalignment of the laser beam on the target, the true non-uniformity of the beam on the array with respect to the string of cells could not be determined. Finally, because the testing was limited to 100 m, the beam uniformity and area was not large enough to cover the entire array. That required partial disassembly of the array to isolate a single string, but the power and the uniformity of the beam on that string were still not determined.

Power was sent via a laser beam to a test article and power produced, but there was no ability to quantify the results. Future tests will certainly overcome these limitations. The lessons learned highlight the need for close collaboration between the suppliers, test operators, researchers, RSO and range staff and laser hazard analyses. Confirmation of beam uniformity at a distance with on-site measurements is essential. This initial testing was most valuable and lays a solid foundation for future tests and demonstrations.

6. REFERENCES

[1] H.W. Brandhorst, Jr., D.R. Forester and M.J. O'Neill, "Effects of the Atmosphere on Laser Transmission to GaAs Solar Cells," *54th International Astronautical Congress*, Bremen, Germany, October 2003.

[2] Smith, M. et. al., *"Laser and Photovoltaic (PV) Wireless Power Transmission Prototype Report 1: PV Cell Characterization"*, U.S. Air Force Research Laboratory AFRL-RX-TY-TR-2011-0100, September 2011, in publication.

[3] Code of Federal Regulations 21CFR1040.1

[4] Code of Federal Regulations 29CFR1910.132 and 1910.133

Appendix A: Laser Test and Hazard Analysis Results

Laser Name	**DILAS***	**Hercules 375****
Laser Parameters		
Wavelength:	810 nm	532 nm
Output Mode:	CW	CW
Average Power:	2550 W	399 mW
Energy Per Pulse:	N/A	N/A
Pulse Duration:	N/A	N/A
PRF:	N/A	N/A
Beam Profile:	Elliptical	Elliptical
Beam Distribution:	TopHat	Not available
Beam Divergence:	3.96 mrad × 2.93 mrad	0.2 mrad × 0.2 mrad
Beam Waist Diameter:	4.6 mm × 6.7 mm	10 mm
Beam Waist Range:	N/A × N/A	N/A × N/A
Output Aperture Diameter:	N/A × N/A	N/A × N/A
Source Size:	N/A × N/A	N/A × N/A
MPE Computations		
Exposure Duration:	10 s	10 s
Exposure Range:	N/A	N/A
MPE (Eye):	1.660e-003 W/cm²	1.000e-003 W/cm²
Limiting Aperture (Eye):	0.7 cm	0.7 cm
Class 1 AEL (Eye):	6.387e-004 W	3.848-004 W
Limiting Aperture (Skin):	0.35 cm	0.35 cm
MPE (Skin):	3.319e-001 W/cm²	1.99e-001 W/cm²
Classification	Class 4	Class IIIb / 4
Hazard Distances and OD Requirements		
Ocular (10 cm, Unaided Viewing, Existing OD = 0)		
Exposure Duration:	10 s	10 s
NOHD:	13,481 ft	63,550 ft
At Viewing Distance:	N/A	N/A
Maximum OD:	6.60	4
At Range OD:	6.60	4
Skin (10 cm, Existing OD = 0		
Exposure Duration:	600 s	600 s
NSHD:	952.77 ft	952.77 ft
At Exposure Distance	10 cm	10 cm
Maximum OD:	4.90	4.90
At Range OD:	4.50	4.50

Laser Name	DILAS*	Hercules 375**
Diffuse Reflection Hazard Analysis		
Laser to Target Range:	100 cm	100 cm
Target Reflectance:	100 %	100 %
Viewing Angle:	0 deg	0 deg
Ocular Hazards		
Exposure Duration:	600 s	600 s
NHZ (Eye):	6.9665 m	6.9665 m
At Viewing Distance:	100 cm	100 cm
OD Required:	1.05	1.05
Skin		
Exposure Duration:	600 s	600 s
NHZ (Skin):	0.49233 m	0.49233 m
At Exposure Distance:	100 cm	100 cm
OD Required:	0.00	0.00
Viewing Conditions:		
Atmos. Attenuation Coeff:	0.0 (1/cm)	0.0 (1/cm)
Aided Viewing Used:	False	False
Optics Transmittance:	N/A	N/A
Optics Objective Diameter:	N/A	N/A
Optics Exit Diameter:	N/A	N/A

*** Laser Report AFRL HEDO Application Framework 2.5.0.69; LHAZ Plugin 5.0.3.3; LTMC Version 3.0.14 / Adapter 5.0.2.15; Tuesday, June 08, 2010**

**** Laser Report; Laserglow Technologies; March 25, 2011**

1. **Appendix B: Eglin Hazard Analysis DILAS Laser**

Calculate the Laser Power Density at the Target (3280 ft) = 2.8 x 10^{-2} W/cm^2 = 280 W/m^2

Inputs

Exposure Parameters	
Use Aided Viewing	False
Calc. Eye Range	**User_Defined**
Eye Range	**3280 ft**
Calc. Skin Range	Standard
Skin Range	10.0 cm
Calc. Eye Exp. Duration	Standard
Eye Exp. Duration	**10 s**
Calc. T_{max}	Standard
T_{max}	**100 s**
Calc. Diffuse Refl. Exp. Duration	Standard
Diffuse Refl. Exp. Duration	600 s
Calc. Skin Exp. Duration	Standard
Skin Exp. Duration	600 s
Existing OD	0
Visibility Conditions	Vacuum, no attenuati
Atmospheric Attenuation	0.0

Laser	
Laser Name	Untitled Laser
Wavelength	**810 nm**
Pulse Mode	CW
Average Power	**2550 W**
Beam Distribution	**TopHat**
Beam Profile	**Elliptical**
Beam Geometry (X)	
Divergence	**3.96 mrad**
Waist_Diameter	**4.6 mm**
External_Waist	False
Extended_Source	Point_Source
Beam Geometry (Y)	
Divergence	**2.93 mrad**
Waist_Diameter	**6.7 mm**
External_Waist	False
Extended_Source	Point_Source

Output

2. Calculate the power radiated on the Photovoltaic Collection Array

Array is 1-ft x 2-ft, which means the area is 2 ft^2 = 0.19 m^2

Radiated power = (280 W/m^2)*(0.19 m^2) = 53.2 W

3. Calculate the Power Reflected by the Photovoltaic Collection Array

   The array reflects 5% of induced power, so reflected power is (53.2 W) * (0.05) = 2.66 W

4. Calculate the hazard distance of the reflected power assuming no refraction

Inputs

Exposure Parameters	
Use Aided Viewing	False
Calc. Eye Range	Standard
Eye Range	0.32808 ft
Calc. Skin Range	Standard
Skin Range	10.0 cm
Calc. Eye Exp. Duration	Standard
Eye Exp. Duration	10 s
Calc. T_{max}	Standard
T_{max}	100 s
Calc. Diffuse Refl. Exp. Duration	Standard
Diffuse Refl. Exp. Duration	600 s
Calc. Skin Exp. Duration	Standard
Skin Exp. Duration	600 s
Existing OD	0
Visibility Conditions	Vacuum, no attenuation
Atmospheric Attenuation	0.0

Laser	
Laser Name	Untitled Laser
Wavelength	810 nm
Pulse Mode	CW
Average Power	2.66 W
Beam Distribution	TopHat
Beam Profile	Elliptical
Beam Geometry (X)	
Divergence	3.96 mrad
Waist_Diameter	2 ft
External_Waist	False
Extended_Source	Point_Source
Beam Geometry (Y)	
Divergence	2.93 mrad
Waist_Diameter	1 ft
External_Waist	False
Extended_Source	Point_Source

Output

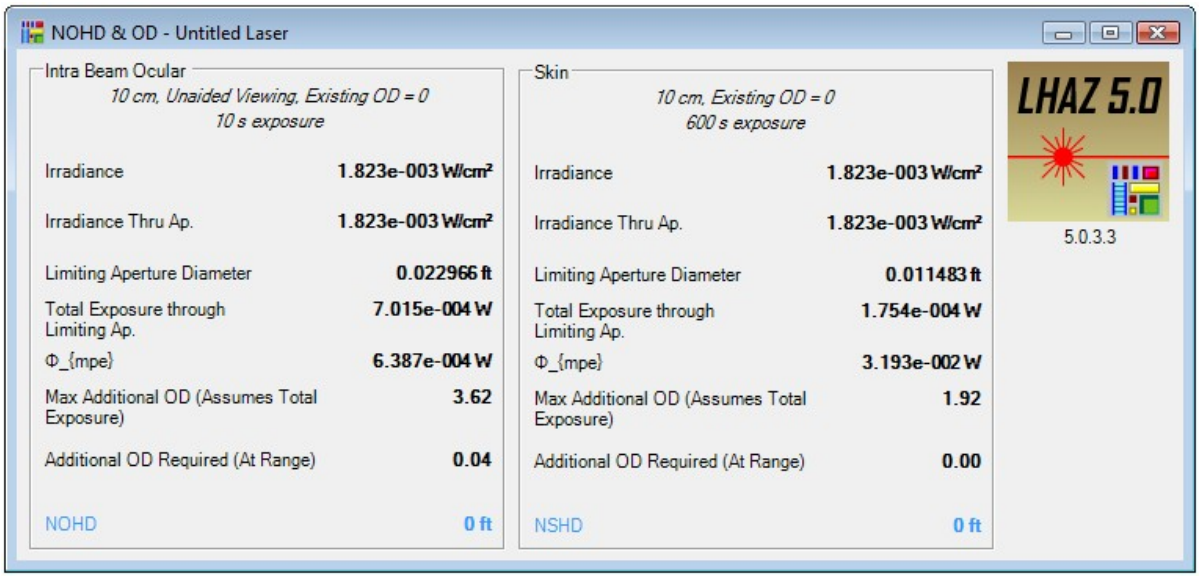

According to the analysis, the NOHD around the collector is 0 ft

LIST OF SYMBOLS, ABBREVIATIONS, AND ACRONYMS

AFRL	Air Force Research Laboratory
AFRL/RH	a unit in the Air Force Research Laboratory
cm^2	square centimeter
CW	continuous wave
eV	electron volt
ft	foot; feet
FWHM	full width at half maximum
GaAs	gallium arsenide
in	inch(es)
Isc	short circuit current of a photovoltaic device
km	kilometer
kW	kilowatts
kW/m^2	power density, kilowatts per square meter
LHAZ	Laser Hazard Analysis software
m	meter(s)
m^2	square meter
MPE (skin)	maximum permissible exposure to the skin
MPE (eye)	maximum permissible exposure to the eye
mrad	milliradians
mV	millivolts
mW	milliwatts
mW/cm^2	power density, milliwatts per square centimeter
NHZ	nominal hazard zone
NIR	near infraRed
nm	nanometer(s)
NOHD	nominal ocular hazard distance
NSHD	nominal skin hazard distance
OD	optical density
Pmax	maximum power of a photovoltaic device
PV	photovoltaic
RSO	Range Safety Officer
Si	silicon
Ti	titanium
TRL	Technology Readiness Level
Voc	open circuit voltage of a photovoltaic device
W	watt
WPT	wireless power transmission